https://doi.org/10.5194/tc-2020-140
Preprint. Discussion started: 2 June 2020

The Cryosphere Discussions

The GRISLI-LSCE contribution to ISMIP6, Part 2: projections of the Antarctic ice sheet evolution by the end of the 21st century

Aurélien Quiquet[1] and Christophe Dumas[1]

[1]Laboratoire des Sciences du Climat et de l'Environnement (LSCE), UMR8212, CEA/CNRS-INSU/UVSQ, Gif-sur-Yvette Cedex, France

Correspondence to: A. Quiquet (aurelien.quiquet@lsce.ipsl.fr)

Abstract.

Of primary societal importance, the ice sheet contribution to global sea level rise over the 21st century remains largely uncertain. In particular, the contribution of the Antarctic ice sheet by 2100 ranges from a few millimetres to more than one metre in the recent literature. The Ice Sheet Model Intercomparison Project for CMIP6 aimed at reducing the uncertainties on the fate of the ice sheets in the future by gathering various ice sheet models in a common framework. While in a companion paper we present the GRISLI-LSCE contribution to ISMIP6-Greenland, we present here the GRISLI-LSCE contribution to ISMIP6-Antarctica. We show that our model is strongly sensitive to the climate forcing used, with a contribution of the Antarctic ice sheet to global sea level rise by 2100 that ranges from -50 mm to +150 mm of sea level equivalent. Future oceanic warming leads to a decrease in thickness of the ice shelves and implies grounding line retreats while increased precipitation partially mitigates the ice sheet contribution to global sea level rise. Most of ice sheet changes over the next century are dampened under low greenhouse gas emission scenarios. Uncertainties related to sub-shelf basal melt induce large differences in simulated grounding line retreats, confirming the importance of this process and its representation in ice sheet models for the projections of the Antarctic ice sheet.

1 Introduction

The Greenland and Antarctic ice sheets are now the largest source for the observed global mean sea level rise behind the thermosteric and the glacier contributions (Nerem et al., 2018). Given its size, the Antarctic ice sheet represents the largest single potential contributor in the future. If the ice sheet has probably displayed a quasi mass-equilibrium in the eighties, it has shown, since then, an important acceleration in mass loss, reaching up to an equivalent of 0.7 mm yr^{-1} of global sea level rise for the last decade (The IMBIE team, 2018; Rignot et al., 2019). The largest changes are observed in West Antarctica with increased ice discharge (Gardner et al., 2018) and increased ice shelf mass loss (Paolo et al., 2015). These recent changes might have already triggered mechanical instabilities (Favier et al., 2014) that could led to an inexorable retreat of the grounding line over large sectors of the ice sheet. If the increased in mass loss is mostly associated with oceanic condition changes, the increased precipitation related to climate change can partially mitigate the ice sheet contribution to sea level rise in the future (Palerme

https://doi.org/10.5194/tc-2020-140
Preprint. Discussion started: 2 June 2020

et al., 2017; Medley and Thomas, 2019).

Despite significant advances in our understanding of ice sheet dynamics (Pattyn et al., 2017), the projected contribution of the Antarctic ice sheet in the future by numerical models remains largely uncertain. Thus, altogether, the uncertainties related to model formulation, parameter choice and external forcing, lead to a wide spread in the magnitude of the Antarctic ice sheet contribution to global sea level rise by 2100, ranging from only a few millimetres to more than one metre (Golledge et al., 2015; Winkelmann et al., 2015; Ritz et al., 2015; DeConto and Pollard, 2016; Schlegel et al., 2018; Edwards et al., 2019; Bulthuis et al., 2019; Levermann et al., 2020). While the different ice sheet models seem to respond consistently to atmospheric changes, oceanic changes translate instead into largely different model responses (Seroussi et al., 2019).

The Ice Sheet Model Intercomparison Project for CMIP6 (ISMIP6, Nowicki et al., 2016), endorsed by the Coupled Model Intercomparison Project – phase 6 (CMIP6), is an international effort that aims at providing estimates of the Greenland and Antarctic ice sheet contributions to global sea level rise by the end of the century. Such intercomparison of models is useful to reduce the uncertainties related to ice sheet dynamics since a variety of ice sheet models have participated in ISMIP6, spanning a range of model complexities and using various initialisation techniques to infer the initial conditions used for the projections. The analysis of the different responses amongst participating ice sheet models is done in Goelzer et al. (2020) for the Greenland ice sheet and in Seroussi et al. (2020) for the Antarctic ice sheet. With the same ice sheet model (GRISLI, Quiquet et al., 2018) and a similar ice sheet initialisation procedure, we participated in both ISMIP6-Greenland and ISMIP6-Antarctica. This paper aims at presenting the GRISLI-LSCE contribution to ISMIP6-Antarctica, while its companion paper (Quiquet and Dumas, submitted) presents the ISMIP6-Greenland contribution. The analysis of a single model for all the different forcing scenarios allows to improve our understanding of the role of the forcing uncertainties in the simulated ice sheet changes.

In Sec. 2 we describe the ice sheet model used for the GRISLI-LSCE contribution and how the model has been initialised. In this section, we also present the ISMIP6 forcing methodology and we describe the complete list of experiments performed. The Antarctic ice sheet simulated by GRISLI for all the different experiments are presented in Sec. 3. Sec. 4 is a broader discussion of these results and we conclude in Sec. 5

2 Methods

2.1 Model and initialisation

The experiments shown here were performed with the 3D thermo-mechanically coupled ice sheet model GRISLI. Solving the mass and momentum conservation equations together with the heat equation, the model computes the evolution of the Antarctic ice sheet geometry and ice physical characteristics. The model is fully described in Quiquet et al. (2018) where the model has been shown to be capable of simulating grounding line migration of the Antarctic ice sheet at the glacial-interglacial timescale.

https://doi.org/10.5194/tc-2020-140
Preprint. Discussion started: 2 June 2020

In the following we only provide the main equations useful for the discussion of the model results.

In GRISLI, the ice sheet is only composed of incompressible ice with a constant and homogeneous density. The mass conservation equation reads

$$\frac{\partial H}{\partial t} = BM - \nabla\left(\bar{\mathbf{U}} H\right) \tag{1}$$

with H the local ice thickness, BM the mass balance and $\bar{\mathbf{U}}$ the vertically averaged horizontal velocity vector. $\nabla\left(\bar{\mathbf{U}} H\right)$ is thus the ice flux divergence.

Velocities are computed using asymptotic *shallow* zero-order approximations, namely the shallow ice approximation (SIA) and the shallow shelf approximations. For the entire grid, the SSA is used as a sliding law (Bueler and Brown, 2009) and the total velocity is the addition of the SIA and the SSA velocities. Floating ice shelves are assumed to have no friction at the base (SSA driven ice flux). Conversely, grounded cold based regions show an infinite friction (SIA driven ice flux). For temperate regions, we assume a linear till below the ice sheet that allows for a viscous deformation (Weertman, 1957):

$$\tau_{\mathbf{b}} = -\beta\, \mathbf{U_b} \tag{2}$$

where τ_b is the basal drag, β is the basal drag coefficient and $\mathbf{U_b}$ is the basal velocity. The basal drag coefficient is spatially variable but constant in time (except in specific cases such as during the inversion procedure).

Calving is based on a simple threshold criterion where ice thickness at the front reaching a minimal value is automatically calved.

For model initialisation, we followed a similar approach as in the initMIP-Antarctica experiments (Seroussi et al., 2019). The initialisation procedure is an iterative method which aims at finding the geographical distribution of the basal drag coefficient (β in Eq. 2) that yields the minimal ice thickness error with respect to the observations. The procedure is described in Le clec'h et al. (2019) and we only provide here a general description. We first compute an ice sheet thermal regime that is in equilibrium with the present-day climate forcing. To this aim, we run a 60 kyr experiment under a perpetual present-day climate forcing and imposing a fixed topography. For this thermal equilibrium experiment, the basal drag coefficient comes from a previous model realisation (Levermann et al., 2020) and is left unchanged. Using the inferred thermal state at the end of the 60 kyr, we performed multiple 120-yr long experiments. Each iteration consists in a first step of 20 years with fixed grounding line position during which the basal drag coefficient is interactively adjusted on a yearly timestep so that it compensates the ice thickness error with respect to the observations (e.g. basal drag reduced for ice thickness overestimation). The second step is a 100 year long experiment with a freely evolving grounding line during which the basal drag remains at its last computed value during the first step. The ice thickness mismatch with respect to the observations at the end of the 100 simulated years is used to modify the basal drag coefficient for the next iteration. This correction consists in having an ice flux on the simulated topography as close as possible to the balance flux on the observed topography Le clec'h et al. (2019). For the experiments shown here we have performed 15 iterations. At the end of the initialisation procedure, we use the last inferred basal drag coefficient together with the corresponding thermal state to run a relaxation experiment of 65 years with a free evolving grounding line.

https://doi.org/10.5194/tc-2020-140
Preprint. Discussion started: 2 June 2020

The simulated ice sheet after this relaxation experiment is used as the initial condition for the historical experiment (*hist*, see Sec. 2.3).

Our reference ice thickness and bedrock topography is the Bedmap2 dataset (Fretwell et al., 2013). This dataset is used as the initial topography for the 65-yr relaxation experiment used to define the initial state for the historical simulation. The ice thickness in Bedmap2 is also used as a target for the iterative initialisation procedure. Our reference present-day surface mass balance comes from RACMO2.3p2 (van Wessem et al., 2018) averaged over 1979-2016. The reference present-day oceanic forcing used to compute the sub-shelf melt rates (more details available in Sec. 2.2) comes from an observational dataset (Jourdain et al., 2019), averaged over 1995-2017. These reference atmospheric and oceanic forcing are used during the initialisation procedure and for the relaxation and control experiments (*ctrl* and *ctrl_proj*, see Sec. 2.3). The geothermal heat flux is the one of Shapiro and Ritzwoller (2004). The model is run on a Cartesian grid at 16 km resolution covering the Antarctic ice sheet using a polar stereographic projection.

2.2 ISMIP6-Antarctica forcing methodology

The ISMIP6-Antarctica working group has elaborated and distributed atmospheric and oceanic forcings in addition to a detailed methodology on how to implement these forcings in individual ice sheet models (Nowicki et al., 2020). Since we have strictly followed the suggested forcing methodology we only provide here the main principles and the reader is invited to refer to Nowicki et al. (2020) for more details.

For ice sheet model projections, the ISMIP6-Antarctica working group has provided a set of yearly climate fields elaborated from various general circulation models (GCMs). The climate fields cover the 1950-2100 period.

- The atmospheric forcing consists in yearly surface mass balance and surface temperature (skin temperature) anomalies with respect to the 1995-2014 mean. The surface mass balance has been computed from the GCM outputs as the total precipitation minus the evaporation and runoff and regridded to the 16 km resolution grid. The anomalies have to be added on top of the reference present-day climatology.
- The oceanic forcing consists in the thermal forcing, i.e. the ambient temperature minus the ambient temperature of the freezing point. In the standard ISMIP6-Antarctica approach, which we follow with GRISLI, the thermal forcing is used to compute sub-shelf melt rates using a non-local quadratic parametrisation as described in Jourdain et al. (2019). For each GCM output, the parametrisation has been calibrated so that it can reproduce the observational dataset around Antarctica. Three estimates for the temperature sensitivity are provided (*low*, *medium* and *high*) for each GCM. In addition, an alternative calibration has been performed for selected GCM. This alternative calibration only uses a subset of the observational data, restricted to the Pine Island glacier basin. This was motivated by the fact that the Pine Island glacier has undergone a substantial grounding line retreat related to an increased sub-shelf melting in the recent years (Jenkins et al., 2018). When calibrated to reproduce the observations for this basin, the parametrisation produces a higher

https://doi.org/10.5194/tc-2020-140
Preprint. Discussion started: 2 June 2020

melt rate response for a given change in thermal forcing than the reference parametrisation calibrated for the whole dataset. The experiments that use this calibration are labelled *PIGL* in the following. As for the standard calibration, three temperature sensitivities are provided, *low*, *medium* and *high*, for the *PIGL* calibration.

Surface melt can generate ice shelf collapse through hydrofracturing. These processes are poorly understood and generally not accounted for in large-scale ice sheet models such as GRISLI. ISMIP6-Antarctica working groups have provided the participants with scenarios for ice shelf collapse in the future following the methodology of Trusel et al. (2015). With these scenarios, the retreat in time of the ice shelf front is imposed. These scenarios are not necessarily used and only the experiments labelled *shelf collapse* (hereafter *SC*) make use of them.

2.3 List of experiments

The ice sheet state (i.e. ice thickness and internal thermomechanical conditions) at the end of the initialisation procedure (Sec. 2.1) is used as initial condition for a control experiment *ctrl* and for the historical simulation *hist*. For the control experiment *ctrl*, the climate forcings (surface temperature, surface mass balance and thermal forcing) are left unchanged for the duration of the experiment at their present-day values used during the initialisation procedure (no anomalies are imposed). The *ctrl* experiment starts in January 1995 and ends in Decembre 2100, even though the time evolution has no incidence on the forcings. Instead, the historical simulation *hist* uses the time varying climate forcing from January 1995 to Decembre 2014. Although it could have been possible to run multiple historical simulations for each GCM output available, it has been asked to participating models to run only one historical simulation using the NorESM1-M climate forcing. NorESM-1-M was chosen because it is one of the CMIP5 models that best reproduce the present-day Antarctic climate change (Barthel et al., 2020).

The different ice sheet projection experiments are all branched to the historical experiment *hist* in Decembre 2014 and they end in Decembre 2100 (86 simulated years). The complete list of experiments in ISMIP6-Antarctica is shown in Tab. 1. Because few CMIP6 models were available when elaborating the ice sheet forcing, most of the experiments make use of CMIP5 models. Four CMIP6 models are nonetheless used (Tier 2). Some climate models were run under two scenarios for future greenhouse gas evolution, a pessimistic scenario (RCP8.5 for CMIP5 models and SSP585 for CMIP6 models) and an optimistic scenario (RCP2.6 for CMIP5 models and SSP126 for CMIP6 models). For each climate forcing, three experiments using different sub-shelf melting rate sensitivity to temperature change (*low*, *medium* and *high*) are performed. In addition, the parametrisation of sub-shelf melt model calibrated against the Pine-Island glacier area (*PIGL*) is used for four CMIP5 models under RCP8.5. The ice shelf collapse scenario related to hydrofracturing is also used for all the climate forcing under the pessimistic scenario. Finally, in order to disentangle the role of atmospheric versus oceanic forcing, a series of experiments also consists in using only one or the other of these forcings.

https://doi.org/10.5194/tc-2020-140
Preprint. Discussion started: 2 June 2020

In order to facilitate the interpretation of the model response to the forcings, an other control experiment, *ctrl_proj*, has also been performed in addition to the *ctrl* experiment. As for the *ctrl* experiment, the climate forcings remain constant with no anomaly with respect to the present-day climate used for the initialisation procedure. However, the *ctrl_proj* starts from the end of the historical simulation in January 2015 where the *ctrl* experiment uses the initial state instead. In doing so, the *ctrl_proj* experiment resembles a projection experiment, except that it uses no anomaly for the climate forcing.

3 Results

While the comparison of the various participating ice sheet models response has been fully described in Seroussi et al. (2020), we aim here at describing the response of one individual model, namely GRISLI, to the various forcings available in ISMIP6-Antarctica.

3.1 Present-day simulated ice sheet

The map of ice thickness error with respect to the observations at the end of the historical simulation is shown in Fig. 1a. These errors are the results of ice thickness changes during the 65 years of relaxation at the end of the initialisation procedure and during the 20 years of the duration of the historical simulation. The differences appear relatively noisy since the model has a tendency to simulate smoother ice thickness gradients than observations. The differences over the East Antarctic plateau are most of the time no greater than a few metres but increases towards the ice margins or in the vicinity of major ice streams (e.g. Amery ice shelf tributaries). In East Antarctica, the Amery and Totten ice shelf regions display the largest error where it can locally approach 500 metres. The ice thickness is generally overestimated in the the Amery region, while it is underestimated in the Totten region. While the errors are relatively localised in East Antarctica, they are more widespread in West Antarctica. There are important ice thickness underestimations in the Getz ice shelf region in the Amundsen sea and upstream the Filchner-Ronne ice shelf grounding line. Except for the Filchner ice shelf, the ice thickness of the ice shelf is slightly underestimated (error lower than 30 metres). The extents of the Ross and Filchner-Ronne ice shelves are overestimated by about 80 km. All together, these discrepancies, integrated over the whole ice sheet, lead to a root mean square error with respect to the observations of about 120 metres (5^{th} lowest error amongst the 21 participating models).

The simulated surface velocity magnitude at the end of the historical simulation is shown in Fig. 2a. The model generally reproduces the location and the magnitude of the observations, depicted in Fig. 2b, even if important errors remain (Fig. 2c). The largest errors are located in fast flowing areas and they can be positive (overestimation) or negative (underestimation). Amongst the largest errors are the large overestimation of the ice velocity for major tributaries of the Ross ice shelf (Mercer and Williams glaciers) and Filchner-Ronne ice shelf (Foundation glacier). Conversely, there is an important underestimation of the ice velocity for the Pine Island ice shelf tributaries. The velocity errors for the grounded part of the ice sheet mostly explain the velocity errors for the floating ice shelves. Thus, the velocity in the Ross ice shelf is largely overestimated while the velocity in the Ronne ice shelf is underestimated. The Amery ice shelf is an exception: the grounded velocity errors are positive

https://doi.org/10.5194/tc-2020-140
Preprint. Discussion started: 2 June 2020

while their floating counterparts are negative. This ice shelf is narrow and very confined with a complex sub-shelf melt pattern which makes it difficult to model for a large scale ice sheet model at 16 km horizontal resolution. All together, the root mean square error with respect to the observations is about 270 m yr^{-1} (3rd largest error amongst the 21 participating models). When computing the error for the logarithm of the velocity in order to reduce the importance of fast flowing regions with respect to slowly flowing regions, the performance of GRISLI with respect to the other participating models slightly improves (6th largest error). This suggests that the model shows the largest disagreement with respect to the observations in fast flowing regions. Our initialisation procedure aims at finding the basal drag coefficient that minimises the ice thickness error with respect to the observations but it does not have any constraints on the simulated velocities. As a result, it is not surprising that we obtain a low RMSE in ice thickness together with a larger RMSE in surface velocities with respect to other ice sheet models that use the velocities in their initialisation procedure.

Even though our initialisation procedure aims at providing a simulated ice sheet in equilibrium with our reference present-day climate, a drift is nonetheless simulated at the century scale. Fig. 1b shows the ice thickness change from 2015 to 2100 in the control experiment *ctrl_proj*. The pattern of ice thickness change resembles the one of the ice thickness error with respect to observations (Fig. 1a). In particular the regions with the largest errors with respect to observations are the one producing the largest ice thickness change in the control simulation. The model drift over the 2015-2100 period can be explained for a large part by the simulated velocity errors with respect to observations (Fig. 2c): thickening (e.g. Pine Island glacier region) is generally associated to an underestimation of the velocity while thinning (e.g. Filchner ice shelf tributaries) is associated to an overestimation of the ice velocity. One exception is the Amery region in East Antarctica where the grounded velocities are overestimated while there is an increase in ice thickness in the control experiment. This inconsistency can be due to surface mass balance errors or an underestimation of the ice flux at the grounding line. Because of compensating errors, the ice thickness change, integrated over the duration of the control experiment, leads to a negligible total ice volume change (less than 1000 km^3). However, the ice volume above floatation shows a negative trend (Fig. 3) which means that there is a mass transfer from the grounded to the floating part of the ice sheet in the control experiment. The model drift in the control experiment *ctrl_proj* in term of surface velocity is shown in Fig. 2. The velocity changes for the grounded areas are generally limited to a few metres except for some ice streams feeding the Ross and Filchner-Ronne ice shelves. Since the ice shelves show a larger velocity magnitude, they also show the largest absolute velocity changes (a few hundred metres locally).

3.2 Ice sheet evolution projections

3.2.1 Ice sheet evolution for CMIP5 models using RCP8.5

The evolution of the ice volume change for the different CMIP5 models under the pessimistic greenhouse gas emission scenario (RCP8.5) and using the sub-shelf melt parametrisation calibrated over the Antarctic wide dataset is shown in Fig. 3. The total ice volume (Fig. 3a) is decreasing for the six CMIP5 models and for most models there is an acceleration in volume loss in the

https://doi.org/10.5194/tc-2020-140
Preprint. Discussion started: 2 June 2020

course of the century. HadGEM2-ES produces the largest ice volume loss (greater than 300000 km^3 in 2100) while CSIRO-Mk3 produces the smallest loss (lower then 50000 km^3). The sub-shelf melt rate sensitivity to temperature change constitutes an important source of uncertainty for the forcings that produce the largest volume loss: for NorESM1-M and HadGEM2-ES the differences between the *low* and *high* oceanic sensitivity corresponds to a volume difference of about 100000 km^3.

The volume change contributing to sea level rise (e.g. above floatation) shows a different evolution than total ice volume (Fig. 3b). While the total ice volume change is always negative, the simulated Antarctic contribution to sea level rise in 2100 for the CMIP5 models can be either positive, e.g. ~60 mm of sea level equivalent (mmSLE) for HadGEM2-ES, or negative, e.g. -45 mmSLE for CCSM4. This means that the ice shelves are systematically reducing in volume while the grounded ice volume has an ambivalent response to the forcings. In addition, except under the HadGEM2-ES forcing, the Antarctic contribution to global sea level rise is always smaller than under the control experiment under perpetual present-day forcing, suggesting increased precipitation in the future. In fact, most GCMs simulate an increase in precipitation in Antarctica related to the projected warming. This has important consequences on the ice sheet integrated surface mass balance and the difference in term of precipitation change amongst the GCMs explains the large spread in simulated Antarctic ice sheet contribution to global sea level rise. Fig. 4 shows the evolution of the surface mass balance (Fig. 4a) and basal mass balance (Fig. 4b) over the next century, integrated over the ice sheet, for the different climate forcings. Despite a considerable interannual variability, the surface mass balance is generally slightly increasing by 15% to 25% (400 to 900 Gt yr^{-1} increase), except for HadGEM2-ES where it shows a slight decrease of about 200 Gt yr^{-1}. Instead, the basal mass balance is always decreasing for the different GCMs leading to an increase in mass loss by about 100% (e.g. 1500 Gt yr^{-1} increase for IPSL-CM5A-MR) to more than 200% (e.g. 5000 Gt yr^{-1} increase for HadGEM2-ES). The lack of precipitation increase in HadGEM2-ES combined with an increase sub-shelf melt explains why this forcing produces the largest Antarctic contribution to future sea level rise.

The spatial pattern of ice thickness change in 2100 with respect to 2015 for a selection of climate forcings is shown in Fig. 5. For this figure, in order to better illustrate the impact of the forcings, the projected ice thickness change has been corrected for the ice thickness change in the control experiment *ctrl_proj* (shown in Fig. 1b). Fig. 5a is for a forcing that produces a large increase in grounded ice volume (CCSM4) under RCP8.5 while Fig. 5b is for a forcing that produces a reduction in both the total and the grounded ice volume (NorESM1-M). For both forcings, the Ross, Filchner-Ronne and Amery ice shelves show important ice thinning, amplified in NorESM1-M with respect to CCSM4. However CCSM4 shows a more pronounced thinning for the Larsen and Fimbul ice shelves, illustrating the spatial heterogeneity amongst the different forcings. Associated with the increased surface mass balance in the course of the century (Fig. 4a), CCSM4 produces a wide spread ice thickening of the grounded ice sheet. When using NorESM1-M this thickening is also presents to a lesser extent but it is also compensated by the thinning that results from the grounding line retreat in some areas (Ross or Totten ice shelves for example). Our model does not simulate important changes in the Pine Island glacier area. This is likely due to the fact that our control experiment tends to produce an ice thickening in this region (Fig. 5b) which tends to stabilise this region, resulting in a smaller sensitivity to oceanic warming.

https://doi.org/10.5194/tc-2020-140
Preprint. Discussion started: 2 June 2020

3.2.2 Ice sheet evolution for CMIP6 models using SSP585

Because CMIP6 models have shown a much larger climate sensitivity than their CMIP5 counterparts (Forster et al., 2020), it is interesting to compare the projected Antarctic ice sheet evolution under the CMIP6 forcings with respect to the CMIP5 experiments discussed previously. In Fig. 6, we show that the CMIP6 forcings produce an ice sheet evolution in the range of what we simulate with the CMIP5 forcings. Three models produce very little ice volume change with an evolution very similar to the CCSM4 CMIP5 model. Only UkESM1 produces a relatively important total ice volume reduction (-250000 km^3) although not associated with a positive ice sheet contribution to sea level rise (about -10 mmSLE). Alike other CMIP5 climate models, the CMIP6 models simulate an increase in the integrated surface mass balance (Fig. 4a) that partly compensate the mass loss due to sub-shelf melting (Fig. 4b). Thus, the new generation of climate projections do not seem to support fundamentally different Antarctic evolution in the future with respect to the previous climate projections.

3.2.3 Ice sheet evolution for RCP2.6 and SSP126

The forcing dataset provided by the ISMIP6-Antarctica working group allows for an evaluation of the impact of the future evolution of the greenhouse gas emission on the Antarctic ice sheet response. In Fig. 7 we show the ice volume change under three climate models that have run for a pessimistic (RCP8.5 or SSP585) and an optimistic (RCP2.6 or SSP126) emission scenario. The total ice volume loss is systematically smaller when using the optimistic scenario. The model that produces the greater volume loss, NorESM1-M, also shows the most pronounced response to the choice of the scenario. For this model, even if the volume loss contributing to global sea level rise remains almost unchanged, there is a drastic reduction in total ice volume loss when using the optimistic scenario. In this case, the ice shelves are able to maintain in the course of the century. For the other two models, IPSL-CM51-MR and CNRM-CM6-1, the main consequence of the use of the optimistic scenario is a reduction of the volume above floatation relative to the volume simulated when using the pessimistic scenario. This is related to the smaller precipitation amount in the colder optimistic scenario. As a result, by the end of the century, the Antarctic ice sheet contribution to global sea level rise is larger (about 30 mmSLE) in the optimistic scenario with respect to the pessimistic one. However, the use of the optimistic scenario systematically produces ice volume evolution closer to the one of the control experiments. This means that the simulated ice sheet changes in the future are dampened with respect to an higher emission scenario.

The impact of the greenhouse gas scenario on the spatial distribution of ice thickness change across 2015-2100 is shown in Fig. 5. On the one hand, NorESM1-M using the RCP8.5 scenario (Fig. 5b) produces drastically thinner ice shelves than when using the RCP2.6 scenario (Fig. 5c). The Ross ice shelf is thus able to maintain until the end of the century with minimal thickness change under the RCP2.6 scenario. On the other hand, the RCP2.6 scenario leads to almost no change in thickness for the grounded parts of the ice sheet whereas under RCP8.5 a slight widespread thickening is simulated, related to increased precipitation.

https://doi.org/10.5194/tc-2020-140
Preprint. Discussion started: 2 June 2020

3.2.4 Ice sheet evolution using the Pine-Island glacier calibrated sub-shelf melt parametrisation

Sub-shelf melt rate computation in ice sheet models is one of the largest source of uncertainty. The standard approach in ISMIP6-Antarctica is a parametrisation largely derived from observational data (Jourdain et al., 2019). However, the choice of the dataset used to calibrate the parametrisation can lead to substantial differences in the sub-shelf melt model. Fig. 8 shows the simulated ice volume change when using the sub-shelf melt parametrisation calibrated to reproduce the mean Antarctic melt rate (reference) or calibrated to reproduce the Pine Island's grounding line melt rate (*PIGL*). The *PIGL* calibration produces higher melt rates and much greater volume loss than the reference calibration. For the medium oceanic sensitivity, the use of the *PIGL* calibration leads to an additional total volume loss of 200000 to 300000 km^3 and an additional contribution to global sea level rise of about 40 to 50 mmSLE with respect to the reference calibration. In addition, with the *PIGL* calibration, the model shows a much larger sensitivity to the oceanic forcing as the difference from a low to a high oceanic sensitivity can be as large as 350000 km^3 (100 mmSLE) when using the CCSM4 forcing.

Amongst the different experiments, the NorESM1-M under rcp8.5 using the *PIGL* calibration for the sub-shelf melt rate with a high oceanic sensitivity produces the largest Antarctic contribution to global sea level rise by 2100. The spatial distribution of ice thickness change over 2015-2100 for this experiment is shown in Fig. 5d. The pattern is similar to the one obtained with the reference sub-shelf melt model (Fig. 5b) but with a much larger decrease in ice thickness. In particular, the grounded line retreats much further inland in the Ross and Filchner-Ronne sectors when using the *PIGL* calibrated sub-shelf melt model with the high oceanic sensitivity.

3.2.5 Ice sheet evolution using the ice shelf collapse scenario

Fig. 9 shows the impact of the imposed ice shelf collapse scenario on the ice volume evolution when using different GCM forcings. Such scenarios lead to an increase in the total volume loss (Fig. 9a) but have, most of the time, a negligible impact on the ice volume contributing to global sea level rise (less than 16 mmSLE in 2100, Fig. 9b). This means that the ice shelf collapse scenarios mostly impact the floating ice volume but, on the century time scale, they do not imply a destabilisation of the grounded ice sheet in our model. The largest response is obtained for CNRM-ESM2 and CNRM-CM6-1. These models show one of the smallest ice mass loss in the future (Fig. 6a) with a limited sub-shelf melt (Fig. 4b). However, they simulate an important atmospheric warming in the future (indirectly visible in the precipitation increase shown in Fig. 4a) that lead to an important ice shelf fracture.

3.2.6 Respective role of atmospheric versus oceanic forcing

Future global warming has ambivalent impacts on the evolution of the Antarctic ice sheet. On the one hand, the Southern Ocean is expected to warm in the future, leading to ice shelf thinning and calving eventually associated to grounding line

https://doi.org/10.5194/tc-2020-140
Preprint. Discussion started: 2 June 2020

destabilisation. On the other hand, the increase in moisture content associated with atmospheric warming can lead to increased precipitation and thickening of the ice sheet. To disentangle the respective role of the oceanic forcing with respect to the atmospheric forcing, we have run the ice sheet model for four climate forcings using alternatively only one or the other of the forcing (ocean only, OO, or atmosphere only, AO). The results in term of volume change is shown in Fig. 10. The AO experiments produce an increase in total ice volume where the OO experiments show a decrease (Fig. 10a). The Antarctic contribution to global sea level rise is systematically smaller than the control experiment *ctrl_proj* for the AO experiments while the OO experiments produce a contribution relatively close to the control experiment *ctrl_proj*, although slightly larger. The CCSM4 model produces the largest surface mass balance increase (Fig. 4a). Interestingly, the Antarctic contribution to sea level rise with this model is almost identical when using the full forcing (Fig. 3b) or when using the atmospheric forcing only (Fig. 10b). This suggests a negligible role of the ocean for this model to explain the Antarctic ice sheet contribution to sea level rise in the future. To a lesser extent this is also the case for the MIROC-ESM-CHEM model. Conversely, the total ice volume change (Fig. 10a) mostly reflects the loss of volume of the ice shelves which, unsurprisingly, mostly responds to the oceanic forcing. The ice shelf volume loss in the OO experiments can be large but it is mostly occurring in the last 20 years of the century. This late response might be a reason why the volume above floatation is not drastically different from the control experiment in the OO experiments.

3.2.7 Simulated change in ice dynamics

The ice sheet surface velocity change in 2100 with respect to 2015 using the NorESM1-M climate forcing with the medium oceanic sensitivity is shown in Fig. 11a. Associated with ice thinning (Fig. 5b), the remaining ice shelves show a large decrease in surface velocity. Grounded ice shows only limited changes in surface velocity with the notable exception of the ice streams feeding the Ross ice shelf that show a substantial acceleration (several hundred metres per year). The acceleration in this area is due to the grounding line retreat simulated by the model under this climate scenario. The pattern of simulated ice velocity change is consistent with results from other ice sheet models (Seroussi et al., 2020) and remains similar for the other forcings: systematic decreased ice shelf velocity and increased grounded velocity only for scenarios that produce a grounding line retreat in the future.

An other way to quantify the dynamic changes over the century is to integrate in time the mass conservation equation (Eq. 1). In doing so, the total ice thickness change from 2015 to 2100 is the superposition of two terms of different natures: the integral of the mass balance related to climate forcings (calving and surface and basal mass balance) and the integral of the ice flux divergence. The integral of the ice flux divergence can be seen as the dynamic contribution to ice thickness change. Such dynamic contribution is shown in Fig. 11b for the NorESM1-M climate forcing with the medium oceanic sensitivity. Generally the dynamic contribution follows the simulated change in surface velocity. In West Antarctica, the dynamic contribution can reach up to more than 50 metres decrease in ice thickness and as such explain most of the simulated ice thickness change shown in Fig. 5b. In East Antarctica there is a widespread very small (a few centimetres) negative dynamic contribution to ice

https://doi.org/10.5194/tc-2020-140
Preprint. Discussion started: 2 June 2020

thickness change (ice thinning) that somehow moderate the ice thickening due to increased precipitation.

4 Discussion

Although in line with results from other ice sheet models participating in ISMIP6-Antarctica, the contribution of the Antarctic ice sheet to global sea level rise simulated by GRISLI is relatively limited. Amongst the different experiments, the largest contribution by 2100 is 150 mmSLE (NorESM1-M *PIGL* with a high oceanic sensitivity) while most experiments produce a contribution no greater than 80 mmSLE. If a relatively moderate Antarctic ice sheet contribution to future sea level rise by 2100 has been suggested in other studies (Bamber et al., 2019; Edwards et al., 2019, e.g.), it seems nonetheless in contradiction with the acceleration in mass loss reported by modern observational techniques Rignot et al. (2019). One reason for this disagreement is that we use a data assimilation procedure that produce an initial condition in quasi-equilibrium with present-day forcing. This methodology is thus not suited to reproduce the recent acceleration in mass loss, particularly important in West Antarctica (Rignot et al., 2019). Assimilation of surface velocities in transient ice sheet simulations are promising methodologies to overcome such limitations (Gillet-Chaulet, 2020) even though they require a complex modelling framework not currently implemented in our ice sheet model. Alternatively, to assess the sensitivity of the model response to the inferred basal drag coefficient, we also perform a set of projections with a uniform perturbation of this parameter after the year 2045. Around its reference value, the perturbation leads mostly to a linear ice volume change (Fig. 12a,b). A uniform reduction of the basal drag coefficient by 30% leads to a 13000 km^3 total volume reduction contributing to about 50 mmSLE in 2100. This means that, with our model, it is unlikely to obtain a significantly different ice volume change for slightly different basal initial conditions. We perform a similar sensitivity experiments but for the enhancement factor and we draw similar conclusion (Fig. 12c,d).

The GRISLI ice sheet model, similarly to other ISMIP6-Antarctica participating models, simulate an ice sheet contribution to global sea level in 2100 that can be either positive or negative, depending on the climate forcing used. This is related to the fact that the climate models simulate an increase in precipitation in the future over Antarctica. An important difference with ISMIP6-Greenland forcing methodology lies in the fact that the atmospheric forcing is much more simplified in ISMIP6-Antarctica. The ISMIP6-Greenland atmospheric scenarios has been elaborated from a regional climate model forced at its boundary by the different GCMs. The atmospheric forcing fields (namely surface temperature and surface mass balance anomalies) are further corrected by the surface elevation changes using time-evolving vertical gradients computed from the regional climate model. Such approach is much more computationally expensive and has been discarded so far for the Antarctic ice sheet where the GCMs anomalies are used directly with no downscaling with a regional climate model and no vertical correction. The use of an approach similar to ISMIP6-Greenland would be an important step forward for the next exercise for Antarctica given the importance of the atmospheric forcing for the Antarctic contribution to future sea level rise.

https://doi.org/10.5194/tc-2020-140
Preprint. Discussion started: 2 June 2020

Although the atmospheric forcing is an important driver for the Antarctic evolution, the oceanic forcing remains the major source of uncertainty for future projections. On the one hand, using a different calibration strategy, the *PIGL* sub-shelf melt model produce a much larger ice sheet retreat than the standard calibration. On the other hand, Seroussi et al. (2020) also show that the ice sheet models that use their own approach to compute the sub-shelf melt in place of the standard ISMIP6-Antarctica melt model are the models that produce generally the largest Antarctic contribution to future sea level rise. Thus, the participating models that use the standard approach all simulate a loss in ice volume above floatation lower than 40 mmSLE in 2100 using NorESM1-M under RCP8.5 with a medium oceanic sensitivity. At the same time, four models that use their own approach simulate a much greater loss, ranging from about 75 to 225 mmSLE, when using the same forcing. This highlights the need for a better understanding of this process, since the various parametrisations used in ice sheet models lead to largely different simulated sub-shelf melt (Favier et al., 2019).

5 Conclusions

In this paper, we have presented the GRISLI-LSCE contribution to ISMIP6-Antarctica, providing a mean to investigate the impact of the climate forcing on one individual ice sheet model. We showed that the volume change simulated by 2100 is strongly dependant on the general circulation model used to force the ice sheet model. On the one hand, the total ice volume is systematically decreasing in the course of the century, primarily because of a reduction in ice shelf volume. The volume loss can be as low as 100000 km^3 to as high as 700000 km^3. On the other hand, the ice volume contributing to sea level rise can be either positive (sea level rise) or negative (see level fall). We simulate a range of ice sheet contribution to global sea level rise by 2100 from about -50 mmSLE to +150 mmSLE. Increased precipitation simulated by most of the climate models in the future tend to increase the grounded ice volume, partly mitigating the effect of ice shelf reduction. By the end of the century, we simulate the largest changes in ice thickness and ice dynamics in the Filchner-Ronne and Ross basin with only moderate changes elsewhere. The geographical pattern of these changes remains mostly consistent amongst the different climate forcings. The CMIP6 climate models do not change drastically the simulated ice sheet in the future with respect to the CMIP5 models. Under low greenhouse gas emission scenario, the Antarctic ice sheet present much less ice volume changes suggesting that the ice sheet volume could be mitigated with a reduction in greenhouse gas emission. The oceanic forcing is a major source of uncertainty since the use of the melt model calibrated against the Pine-Island glacier data instead of the standard calibration produces a much faster ice shelf retreat and, as a result, a larger ice sheet volume contribution to sea level rise in the future. This process has to be carefully assessed when performing future projections of the Antarctic ice sheet.

6 Data availability

The GRISLI outputs from the experiments described in this paper are available on the zenodo repository with digital object identifier 10.5281/zenodo.3819782. The outputs in the zenodo repository are the standard GRISLI outputs on the native 16 km

https://doi.org/10.5194/tc-2020-140
Preprint. Discussion started: 2 June 2020

grid and, as a result, they may slightly differ from the post-processed outputs available on the official CMIP6 archive on the Earth System Grid Federation (ESGF). In order to document CMIP6's scientific impact and enable ongoing support of CMIP, users are obligated to acknowledge CMIP6, the participating modelling groups, and the ESGF centres (see details on the CMIP Panel website at http://www.wcrp- climate.org/index.php/wgcm-cmip/about-cmip). The forcing datasets are available through the ISMIP6 wiki and are also made publicly available via https://doi.org/xxx.

Acknowledgements. We thank the Climate and Cryosphere (CliC) effort, which provided support for ISMIP6 through sponsoring of workshops, hosting the ISMIP6 website and wiki, and promoted ISMIP6. We acknowledge the World Climate Research Programme, which, through its Working Group on Coupled Modelling, coordinated and promoted CMIP5 and CMIP6. We thank the climate modeling groups for producing and making available their model output, the Earth System Grid Federation (ESGF) for archiving the CMIP data and providing access, the University at Buffalo for ISMIP6 data distribution and upload, and the multiple funding agencies who support CMIP5 and CMIP6 and ESGF. We thank the ISMIP6 steering committee, the ISMIP6 model selection group and ISMIP6 dataset preparation group for their continuous engagement in defining ISMIP6. This is ISMIP6 contribution No X.

https://doi.org/10.5194/tc-2020-140
Preprint. Discussion started: 2 June 2020

References

Bamber, J. L., Oppenheimer, M., Kopp, R. E., Aspinall, W. P., and Cooke, R. M.: Ice sheet contributions to future sea-level rise from structured expert judgment, Proceedings of the National Academy of Sciences, 116, 11 195–11 200, doi:10.1073/pnas.1817205116, 2019.

Barthel, A., Agosta, C., Little, C. M., Hattermann, T., Jourdain, N. C., Goelzer, H., Nowicki, S., Seroussi, H., Straneo, F., and Bracegirdle, T. J.: CMIP5 model selection for ISMIP6 ice sheet model forcing: Greenland and Antarctica, The Cryosphere, 14, 855–879, doi:https://doi.org/10.5194/tc-14-855-2020, 2020.

Bueler, E. and Brown, J.: Shallow shelf approximation as a "sliding law" in a thermomechanically coupled ice sheet model, Journal of Geophysical Research: Earth Surface, 114, F03 008, doi:10.1029/2008JF001179, 2009.

Bulthuis, K., Arnst, M., Sun, S., and Pattyn, F.: Uncertainty quantification of the multi-centennial response of the Antarctic ice sheet to climate change, The Cryosphere, 13, 1349–1380, doi:10.5194/tc-13-1349-2019, 2019.

DeConto, R. M. and Pollard, D.: Contribution of Antarctica to past and future sea-level rise, Nature, 531, 591, doi:10.1038/nature17145, 2016.

Edwards, T. L., Brandon, M. A., Durand, G., Edwards, N. R., Golledge, N. R., Holden, P. B., Nias, I. J., Payne, A. J., Ritz, C., and Wernecke, A.: Revisiting Antarctic ice loss due to marine ice-cliff instability, Nature, 566, 58–64, doi:10.1038/s41586-019-0901-4, 2019.

Favier, L., Durand, G., Cornford, S. L., Gudmundsson, G. H., Gagliardini, O., Gillet-Chaulet, F., Zwinger, T., Payne, A. J., and Brocq, A. M. L.: Retreat of Pine Island Glacier controlled by marine ice-sheet instability, Nature Climate Change, 4, 117, doi:10.1038/nclimate2094, 2014.

Favier, L., Jourdain, N. C., Jenkins, A., Merino, N., Durand, G., Gagliardini, O., Gillet-Chaulet, F., and Mathiot, P.: Assessment of sub-shelf melting parameterisations using the ocean–ice-sheet coupled model NEMO(v3.6)–Elmer/Ice(v8.3), Geoscientific Model Development, 12, 2255–2283, doi:https://doi.org/10.5194/gmd-12-2255-2019, 2019.

Forster, P. M., Maycock, A. C., McKenna, C. M., and Smith, C. J.: Latest climate models confirm need for urgent mitigation, Nature Climate Change, 10, 7–10, doi:10.1038/s41558-019-0660-0, 2020.

Fretwell, P., Pritchard, H. D., Vaughan, D. G., Bamber, J. L., Barrand, N. E., Bell, R., Bianchi, C., Bingham, R. G., Blankenship, D. D., Casassa, G., Catania, G., Callens, D., Conway, H., Cook, A. J., Corr, H. F. J., Damaske, D., Damm, V., Ferraccioli, F., Forsberg, R., Fujita, S., Gim, Y., Gogineni, P., Griggs, J. A., Hindmarsh, R. C. A., Holmlund, P., Holt, J. W., Jacobel, R. W., Jenkins, A., Jokat, W., Jordan, T., King, E. C., Kohler, J., Krabill, W., Riger-Kusk, M., Langley, K. A., Leitchenkov, G., Leuschen, C., Luyendyk, B. P., Matsuoka, K., Mouginot, J., Nitsche, F. O., Nogi, Y., Nost, O. A., Popov, S. V., Rignot, E., Rippin, D. M., Rivera, A., Roberts, J., Ross, N., Siegert, M. J., Smith, A. M., Steinhage, D., Studinger, M., Sun, B., Tinto, B. K., Welch, B. C., Wilson, D., Young, D. A., Xiangbin, C., and Zirizzotti, A.: Bedmap2: improved ice bed, surface and thickness datasets for Antarctica, The Cryosphere, 7, 375–393, doi:10.5194/tc-7-375-2013, 2013.

Gardner, A. S., Moholdt, G., Scambos, T., Fahnstock, M., Ligtenberg, S., Broeke, M. v. d., and Nilsson, J.: Increased West Antarctic and unchanged East Antarctic ice discharge over the last 7 years, The Cryosphere, 12, 521–547, doi:https://doi.org/10.5194/tc-12-521-2018, 2018.

Gillet-Chaulet, F.: Assimilation of surface observations in a transient marine ice sheet model using an ensemble Kalman filter, The Cryosphere, 14, 811–832, doi:https://doi.org/10.5194/tc-14-811-2020, 2020.

Goelzer, H., Nowicki, S., Payne, A., Larour, E., Seroussi, H., Lipscomb, W. H., Gregory, J., Abe-Ouchi, A., Shepherd, A., Simon, E., Agosta, C., Alexander, P., Aschwanden, A., Barthel, A., Calov, R., Chambers, C., Choi, Y., Cuzzone, J., Dumas, C., Edwards, T., Felikson, D.,

Fettweis, X., Golledge, N. R., Greve, R., Humbert, A., Huybrechts, P., Clec'h, S. L., Lee, V., Leguy, G., Little, C., Lowry, D. P., Morlighem, M., Nias, I., Quiquet, A., Rückamp, M., Schlegel, N.-J., Slater, D., Smith, R., Straneo, F., Tarasov, L., Wal, R. v. d., and Broeke, M. v. d.: The future sea-level contribution of the Greenland ice sheet: a multi-model ensemble study of ISMIP6, The Cryosphere Discussions, pp. 1–43, doi:https://doi.org/10.5194/tc-2019-319, 2020.

Golledge, N. R., Kowalewski, D. E., Naish, T. R., Levy, R. H., Fogwill, C. J., and Gasson, E. G. W.: The multi-millennial Antarctic commitment to future sea-level rise, Nature, 526, 421, doi:10.1038/nature15706, 2015.

Jenkins, A., Shoosmith, D., Dutrieux, P., Jacobs, S., Kim, T. W., Lee, S. H., Ha, H. K., and Stammerjohn, S.: West Antarctic Ice Sheet retreat in the Amundsen Sea driven by decadal oceanic variability, Nature Geoscience, 11, 733–738, doi:10.1038/s41561-018-0207-4, 2018.

Jourdain, N. C., Asay-Davis, X., Hattermann, T., Straneo, F., Seroussi, H., Little, C. M., and Nowicki, S.: A protocol for calculating basal melt rates in the ISMIP6 Antarctic ice sheet projections, The Cryosphere Discussions, pp. 1–33, doi:https://doi.org/10.5194/tc-2019-277, https://www.the-cryosphere-discuss.net/tc-2019-277/, 2019.

Le clec'h, S., Quiquet, A., Charbit, S., Dumas, C., Kageyama, M., and Ritz, C.: A rapidly converging initialisation method to simulate the present-day Greenland ice sheet using the GRISLI ice sheet model (version 1.3), Geoscientific Model Development, 12, 2481–2499, doi:10.5194/gmd-12-2481-2019, 2019.

Levermann, A., Winkelmann, R., Albrecht, T., Goelzer, H., Golledge, N. R., Greve, R., Huybrechts, P., Jordan, J., Leguy, G., Martin, D., Morlighem, M., Pattyn, F., Pollard, D., Quiquet, A., Rodehacke, C., Seroussi, H., Sutter, J., Zhang, T., Breedam, J. V., Calov, R., DeConto, R., Dumas, C., Garbe, J., Gudmundsson, G. H., Hoffman, M. J., Humbert, A., Kleiner, T., Lipscomb, W. H., Meinshausen, M., Ng, E., Nowicki, S. M. J., Perego, M., Price, S. F., Saito, F., Schlegel, N.-J., Sun, S., and Wal, R. S. W. v. d.: Projecting Antarctica's contribution to future sea level rise from basal ice shelf melt using linear response functions of 16 ice sheet models (LARMIP-2), Earth System Dynamics, 11, 35–76, doi:https://doi.org/10.5194/esd-11-35-2020, 2020.

Medley, B. and Thomas, E. R.: Increased snowfall over the Antarctic Ice Sheet mitigated twentieth-century sea-level rise, Nature Climate Change, 9, 34–39, doi:10.1038/s41558-018-0356-x, 2019.

Nerem, R. S., Beckley, B. D., Fasullo, J. T., Hamlington, B. D., Masters, D., and Mitchum, G. T.: Climate-change–driven accelerated sea-level rise detected in the altimeter era, Proceedings of the National Academy of Sciences, 115, 2022–2025, doi:10.1073/pnas.1717312115, 2018.

Nowicki, S., Payne, A. J., Goelzer, H., Seroussi, H., Lipscomb, W. H., Abe-Ouchi, A., Agosta, C., Alexander, P., Asay-Davis, X. S., Barthel, A., Bracegirdle, T. J., Cullather, R., Felikson, D., Fettweis, X., Gregory, J., Hatterman, T., Jourdain, N. C., Kuipers Munneke, P., Larour, E., Little, C. M., Morlinghem, M., Nias, I., Shepherd, A., Simon, E., Slater, D., Smith, R., Straneo, F., Trusel, L. D., Broeke, M. R. v. d., and Wal, R. v. d.: Experimental protocol for sealevel projections from ISMIP6 standalone ice sheet models, The Cryosphere Discussions, pp. 1–40, doi:https://doi.org/10.5194/tc-2019-322, 2020.

Nowicki, S. M. J., Payne, A., Larour, E., Seroussi, H., Goelzer, H., Lipscomb, W., Gregory, J., Abe-Ouchi, A., and Shepherd, A.: Ice Sheet Model Intercomparison Project (ISMIP6) contribution to CMIP6, Geosci. Model Dev., 9, 4521–4545, doi:10.5194/gmd-9-4521-2016, 2016.

Palerme, C., Genthon, C., Claud, C., Kay, J. E., Wood, N. B., and L'Ecuyer, T.: Evaluation of current and projected Antarctic precipitation in CMIP5 models, Climate Dynamics, 48, 225–239, doi:10.1007/s00382-016-3071-1, 2017.

Paolo, F. S., Fricker, H. A., and Padman, L.: Volume loss from Antarctic ice shelves is accelerating, Science, 348, 327–331, doi:10.1126/science.aaa0940, 2015.

Pattyn, F., Favier, L., Sun, S., and Durand, G.: Progress in Numerical Modeling of Antarctic Ice-Sheet Dynamics, Current Climate Change Reports, 3, 174–184, doi:10.1007/s40641-017-0069-7, 2017.

Quiquet, A. and Dumas, C.: The GRISLI-LSCE contribution to ISMIP6, Part 1: projections of the Greenland ice sheet evolution by the end of the 21st century, The Cryosphere Discussion, submitted.

Quiquet, A., Dumas, C., Ritz, C., Peyaud, V., and Roche, D. M.: The GRISLI ice sheet model (version 2.0): calibration and validation for multi-millennial changes of the Antarctic ice sheet, Geoscientific Model Development, 11, 5003–5025, doi:10.5194/gmd-11-5003-2018, 2018.

Rignot, E., Mouginot, J., and Scheuchl, B.: Ice Flow of the Antarctic Ice Sheet, Science, 333, 1427–1430, doi:10.1126/science.1208336, 2011.

Rignot, E., Mouginot, J., Scheuchl, B., van den Broeke, M., van Wessem, M. J., and Morlighem, M.: Four decades of Antarctic Ice Sheet mass balance from 1979–2017, Proceedings of the National Academy of Sciences, 116, 1095–1103, doi:10.1073/pnas.1812883116, 2019.

Ritz, C., Edwards, T. L., Durand, G., Payne, A. J., Peyaud, V., and Hindmarsh, R. C. A.: Potential sea-level rise from Antarctic ice-sheet instability constrained by observations, Nature, 528, 115–118, doi:10.1038/nature16147, 2015.

Schlegel, N.-J., Seroussi, H., Schodlok, M. P., Larour, E. Y., Boening, C., Limonadi, D., Watkins, M. M., Morlighem, M., and Broeke, M. R. v. d.: Exploration of Antarctic Ice Sheet 100-year contribution to sea level rise and associated model uncertainties using the ISSM framework, The Cryosphere, 12, 3511–3534, doi:https://doi.org/10.5194/tc-12-3511-2018, 2018.

Seroussi, H., Nowicki, S., Simon, E., Abe-Ouchi, A., Albrecht, T., Brondex, J., Cornford, S., Dumas, C., Gillet-Chaulet, F., Goelzer, H., Golledge, N., Gregory, J., Greve, R., Hoffman, M., Humbert, A., Huybrechts, P., Kleiner, T., Larour, E., Leguy, G., Lipscomb, W. H., Lowry, D., Mengel, M., Morlighem, M., Pattyn, F., Payne, A., Pollard, D., Price, S., Quiquet, A., Reerink, T., Reese, R., Rodehacke, C., Schlegel, N.-J., Shepherd, A., Sun, S., Sutter, J., Breedam, J. V., Wal, R. v. d., Winkelmann, R., and Zhang, T.: initMIP-Antarctica: an ice sheet model initialization experiment of ISMIP6, The Cryosphere, 13, 1441–1471, doi:10.5194/tc-13-1441-2019, 2019.

Seroussi, H., Nowicki, S., Payne, A. J., Goelzer, H., Lipscomb, W. H., Abe Ouchi, A., Agosta, C., Albrecht, T., Asay-Davis, X., Barthel, A., Calov, R., Cullather, R., Dumas, C., Gladstone, R., Golledge, N., Gregory, J. M., Greve, R., Hatterman, T., Hoffman, M. J., Humbert, A., Huybrechts, P., Jourdain, N. C., Kleiner, T., Larour, E., Leguy, G. R., Lowry, D. P., Little, C. M., Morlighem, M., Pattyn, F., Pelle, T., Price, S. F., Quiquet, A., Reese, R., Schlegel, N.-J., Shepherd, A., Simon, E., Smith, R. S., Straneo, F., Sun, S., Trusel, L. D., Breedam, J. V., Wal, R. S. W. v. d., Winkelmann, R., Zhao, C., Zhang, T., and Zwinger, T.: ISMIP6 Antarctica: a multi-model ensemble of the Antarctic ice sheet evolution over the 21st century, The Cryosphere Discussions, pp. 1–54, doi:https://doi.org/10.5194/tc-2019-324, 2020.

Shapiro, N. M. and Ritzwoller, M. H.: Inferring surface heat flux distributions guided by a global seismic model: particular application to Antarctica, Earth and Planetary Science Letters, 223, 213–224, doi:10.1016/j.epsl.2004.04.011, 2004.

The IMBIE team: Mass balance of the Antarctic Ice Sheet from 1992 to 2017, Nature, 558, 219–222, doi:10.1038/s41586-018-0179-y, 2018.

Trusel, L. D., Frey, K. E., Das, S. B., Karnauskas, K. B., Munneke, P. K., Meijgaard, E. v., and Broeke, M. R. v. d.: Divergent trajectories of Antarctic surface melt under two twenty-first-century climate scenarios, Nature Geoscience, 8, 927–932, doi:10.1038/ngeo2563, 2015.

van Wessem, J. M., Berg, W. J. v. d., Noël, B. P. Y., Meijgaard, E. v., Amory, C., Birnbaum, G., Jakobs, C. L., Krüger, K., Lenaerts, J. T. M., Lhermitte, S., Ligtenberg, S. R. M., Medley, B., Reijmer, C. H., Tricht, K. v., Trusel, L. D., Ulft, L. H. v., Wouters, B., Wuite, J., and Broeke, M. R. v. d.: Modelling the climate and surface mass balance of polar ice sheets using RACMO2 – Part 2: Antarctica (1979–2016), The Cryosphere, 12, 1479–1498, doi:https://doi.org/10.5194/tc-12-1479-2018, 2018.

Weertman, J.: On the Sliding of Glaciers, Journal of Glaciology, 3, 33–38, doi:10.3189/S0022143000024709, 1957.

https://doi.org/10.5194/tc-2020-140
Preprint. Discussion started: 2 June 2020

Winkelmann, R., Levermann, A., Ridgwell, A., and Caldeira, K.: Combustion of available fossil fuel resources sufficient to eliminate the Antarctic Ice Sheet, Science Advances, 1, e1500 589, doi:10.1126/sciadv.1500589, 2015.

https://doi.org/10.5194/tc-2020-140
Preprint. Discussion started: 2 June 2020

The Cryosphere Discussions
Open Access
EGU

Table 1. List of ISMIP6-Antarctica experiments performed in this work. The three oceanic sensitivities are low, medium (med) and high. The experiments that use the sub-shelf melt parametrisation calibrated against the Pine Island glacier data are labelled *PIGL*. The experiments that use the imposed ice shelf collapse scenario due to hydrofracturing are labelled *SC*.

exp_id	scenario	GCM	Ocean	
exp05	RCP8.5	NorESM1-M	Med	Core experiments – Tier 1
exp06	RCP8.5	MIROC-ESM-CHEM	Med	
exp07	RCP2.6	NorESM1-M	Med	
exp08	RCP8.5	CCSM4	Med	
exp09	RCP8.5	NorESM1-M	High	
exp10	RCP8.5	NorESM1-M	Low	
exp12	RCP8.5	CCSM4	*SC* Med	
exp13	RCP8.5	NorESM1-M	*PIGL* Med	
expa05	RCP8.5	HadGEM2-RS	Med	Extended ensemble – Tier 2
expa06	RCP8.5	CSIRO-Mk3	Med	
expa07	RCP8.5	IPSL-CM5-MR	Med	
expa08	RCP2.6	IPSL-CM5-MR	Med	
expb06	SSP585	CNRM-CM6-1	Med	CMIP6 extension – Tier 2
expb07	SSP126	CNRM-CM6-1	Med	
expb08	SSP585	UKESM1-0-LL	Med	
expb09	SSP585	CESM2	Med	
expb10	SSP585	CNRM-ESM2-1	Med	
expc01	RCP8.5	NorESM1-M AO	Med	Ocean only (OO) and Atmos. only (AO) – Tier 3
expc03	RCP8.5	NorESM1-M OO	Med	
expc04	RCP8.5	MIROC-ESM-CHEM AO	Med	
expc06	RCP8.5	MIROC-ESM-CHEM OO	Med	
expc07	RCP2.6	NorESM1-M AO	Med	
expc09	RCP2.6	NorESM1-M OO	Med	
expc10	RCP8.5	CCSM4 AO	Med	
expc12	RCP8.5	CCSM4 OO	Med	

exp_id	scenario	GCM	Ocean	
expd01	RCP8.5	MIROC-ESM-CHEM	High	Ocean sensitivity – Tier 3
expd02	RCP8.5	MIROC-ESM-CHEM	Low	
expd03	RCP2.6	NorESM1-M	High	
expd04	RCP2.6	NorESM1-M	Low	
expd05	RCP8.5	CCSM4	High	
expd06	RCP8.5	CCSM4	Low	
expd07	RCP8.5	HadGEM2-RS	High	
expd08	RCP8.5	HadGEM2-RS	Low	
expd09	RCP8.5	CSIRO-Mk3	High	
expd10	RCP8.5	CSIRO-Mk3	Low	
expd11	RCP8.5	IPSL-CM5-MR	High	
expd12	RCP8.5	IPSL-CM5-MR	Low	
expd13	SSP585	CNRM-CM6-1	High	
expd14	SSP585	CNRM-CM6-1	Low	
expd15	SSP585	UKESM1-0-LL	High	
expd16	SSP585	UKESM1-0-LL	Low	
expd17	SSP585	CESM2	High	
expd18	SSP585	CESM2	Low	
expd51	RCP8.5	NorESM1-M	*PIGL* Low	
expd52	RCP8.5	NorESM1-M	*PIGL* High	
expd53	RCP8.5	MIROC-ESM-CHEM	*PIGL* Med	
expd54	RCP8.5	MIROC-ESM-CHEM	*PIGL* Low	
expd55	RCP8.5	MIROC-ESM-CHEM	*PIGL* High	
expd56	RCP8.5	CCSM4	*PIGL* Med	
expd57	RCP8.5	CCSM4	*PIGL* Low	
expd58	RCP8.5	CCSM4	*PIGL* High	
expe06	RCP8.5	NorESM1-M	*SC* Med	Ice shelf collapse – Tier 3
expe07	RCP8.5	MIROC-ESM-CHEM	*SC* Med	
expe08	RCP8.5	HadGEM2-RS	*SC* Med	
expe09	RCP8.5	CSIRO-Mk3	*SC* Med	
expe10	RCP8.5	IPSL-CM5-MR	*SC* Med	
expe15	SSP585	CNRM-CM6-1	*SC* Med	
expe16	SSP585	UKESM1-0-LL	*SC* Med	
expe17	SSP585	CESM2	*SC* Med	
expe18	SSP585	CNRM-ESM2-1	*SC* Med	

https://doi.org/10.5194/tc-2020-140
Preprint. Discussion started: 2 June 2020

The Cryosphere
Discussions
Open Access
EGU

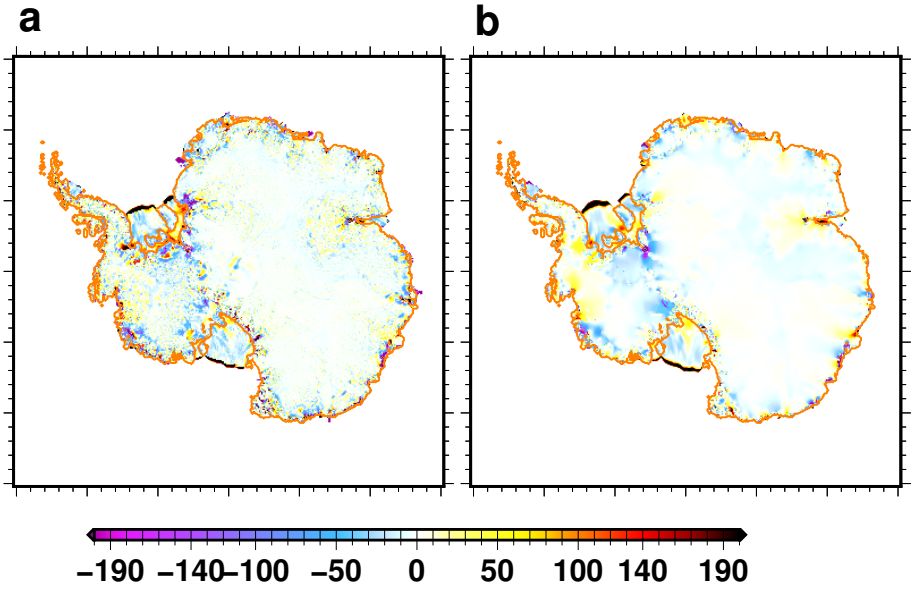

Figure 1. Ice thickness difference: **(a)** end of the historical experiment *hist* with respect to observations (Fretwell et al., 2013); **(b)** end of the control experiment *ctrl_proj* with respect to the end of the historical experiment *hist*. The orange line shows the present-day grounded line.

https://doi.org/10.5194/tc-2020-140
Preprint. Discussion started: 2 June 2020

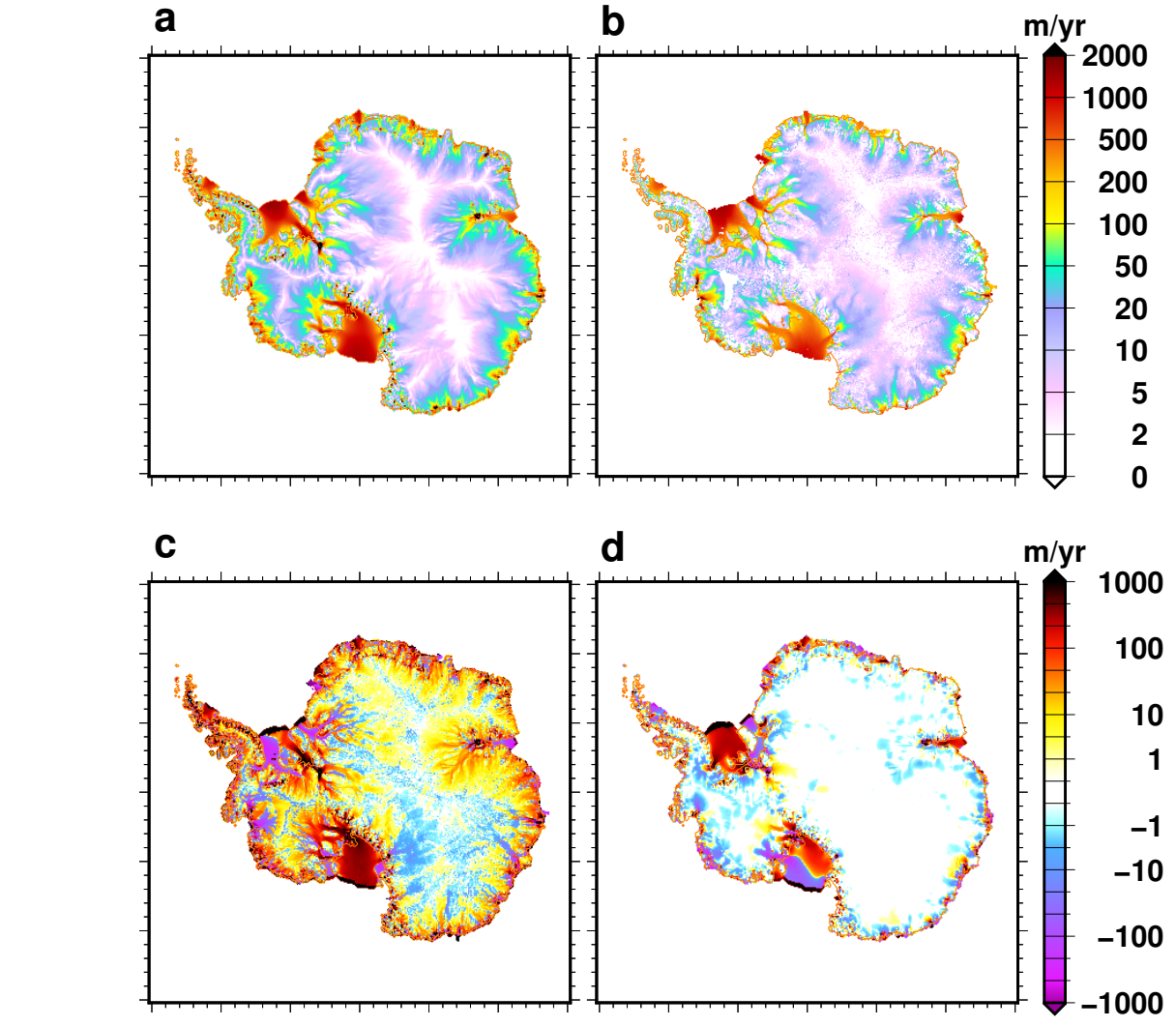

Figure 2. Surface velocity magnitude: **(a)** simulated at the end (2011-2015) of the historical experiment *hist*; **(b)** in the observational datasets of Rignot et al. (2011); **(c)** difference between (a) and (b). The surface velocity magnitude change from 2011-2015 to 2096-2100 in the control experiment *ctrl_proj* is shown in **d**. We use a 5 year mean for the simulated velocity to reduce the impact of interannual variability.

https://doi.org/10.5194/tc-2020-140
Preprint. Discussion started: 2 June 2020

The Cryosphere Discussions
Open Access
EGU

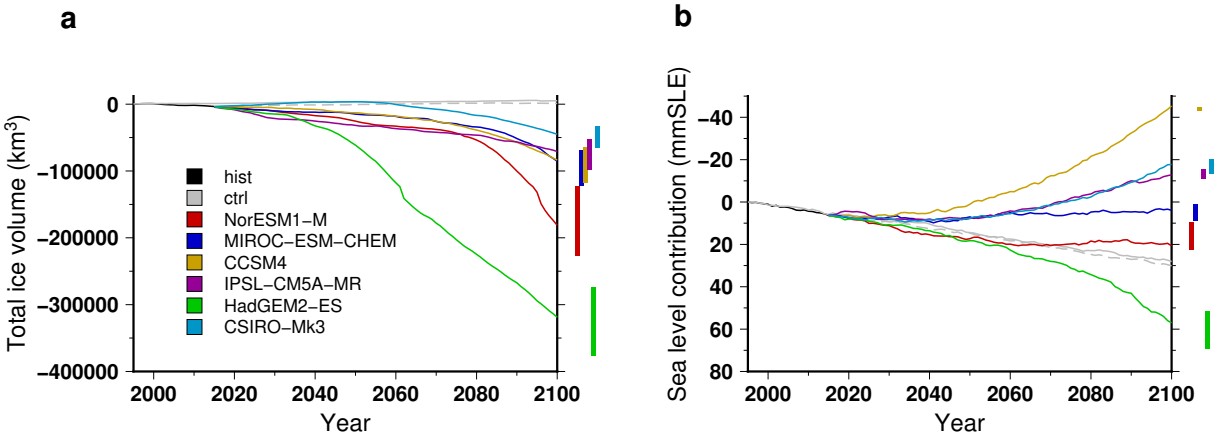

Figure 3. Simulated ice volume change for the historical simulation *hist* (1995-2015), the control experiments *ctrl* (solid grey lines) and *ctrl_proj* (dashed grey lines) and the projections under the different CMIP5 forcings using the RCP8.5 scenario and the medium oceanic sensitivity: **(a)** total ice volume change and **(b)** ice volume contributing to sea level rise. For each projection experiment the vertical bar shows the minimal and maximal volume change associated with the oceanic forcing sensitivity to temperature change (*low* and *high*).

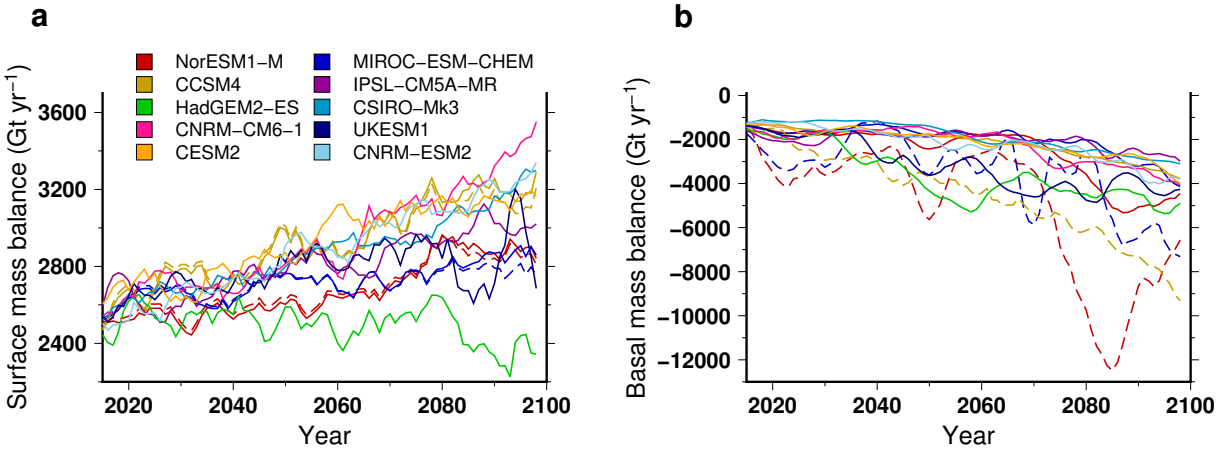

Figure 4. Simulated surface mass balance **(a)** and basal mass balance **(b)**, integrated over the ice sheet, for different CMIP5 and CMIP6 climate forcings using the RCP8.5 scenario and SSP585 scenario, respectively. The projection experiments shown in this figure use the medium oceanic sensitivity. The solid lines stand for the experiments that use the sub-shelf melting parametrisation calibrated against all the Antarctic data while the dashed lines are for the experiments that use a parametrisation calibrated against Pine-Island area data only. For this figure we use a 5-year running mean in order to smooth the interannual variability.

https://doi.org/10.5194/tc-2020-140
Preprint. Discussion started: 2 June 2020

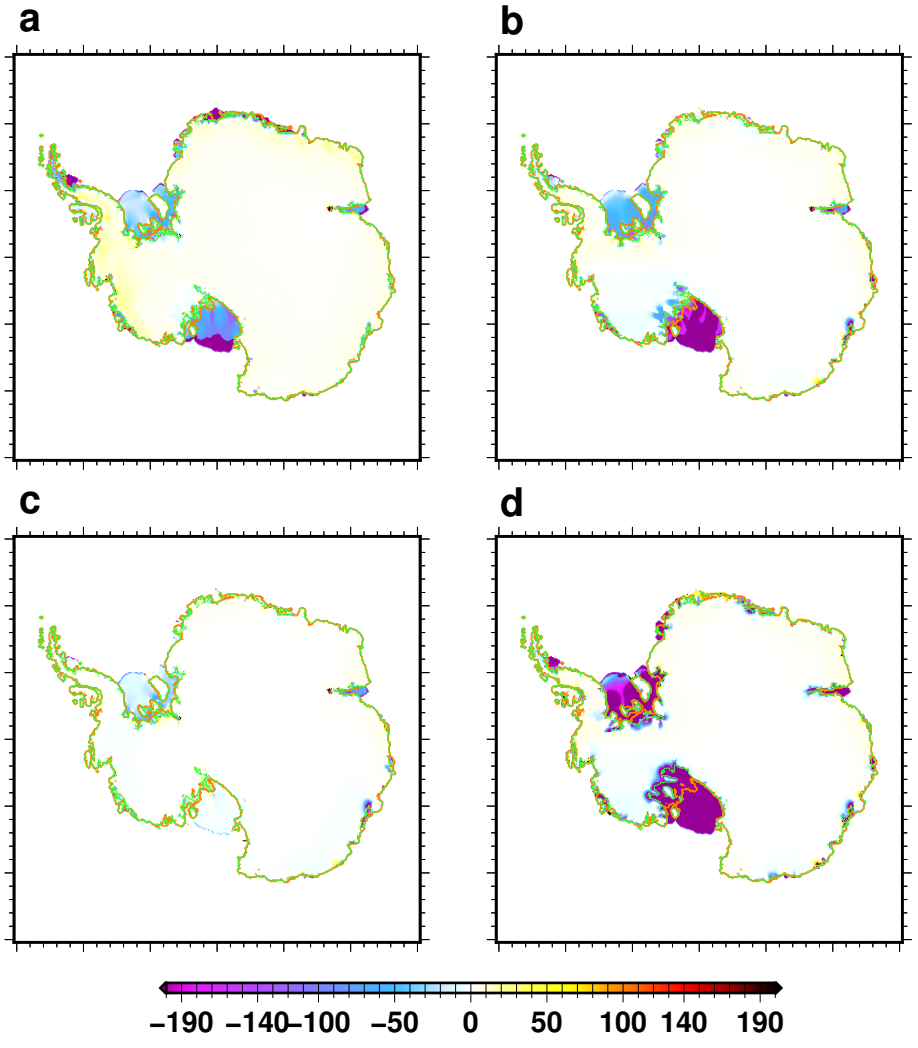

Figure 5. Simulated ice thickness change (2100 - 2015) for: **(a)** CESM2 (SSP585); **(b)** NorESM1-M (RCP8.5); **(c)** NorESM1-M (RCP2.6) and; **(d)** NorESM1-M (RCP8.5) *PIGL*. The orange line shows the the present-day grounded line and the light green line represents its simulated position in 2100. The medium oceanic sensitivity has been used here, except for the *PIGL* experiment (d) for which we use the high oceanic sensitivity. The ice thickness change shown here is corrected for the ice thickness change (2100-2015) in the control experiment *ctrl_proj*.

https://doi.org/10.5194/tc-2020-140
Preprint. Discussion started: 2 June 2020

The Cryosphere Discussions
Open Access
EGU

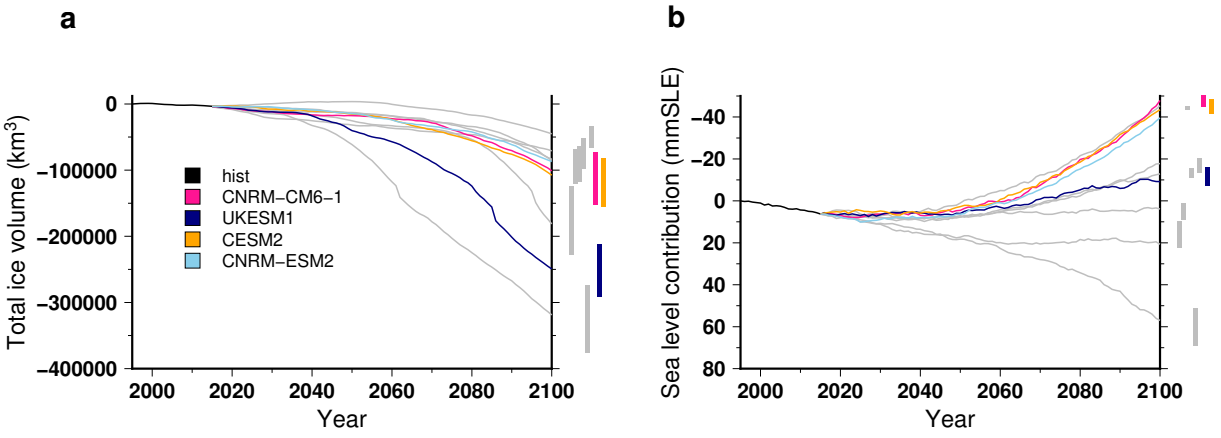

Figure 6. Simulated ice volume change for the historical experiment *hist* (1995-2015) and the projections under the different CMIP6 forcings using the SSP585 scenario and the medium oceanic sensitivity: **(a)** total ice volume change and **(b)** ice volume contributing to sea level rise. For each projection experiment the vertical bar shows the minimal and maximal volume change associated with the oceanic forcing sensitivity to temperature change (*low* and *high*). The grey lines are the volume change under the CMIP5 forcings shown in Fig. 3.

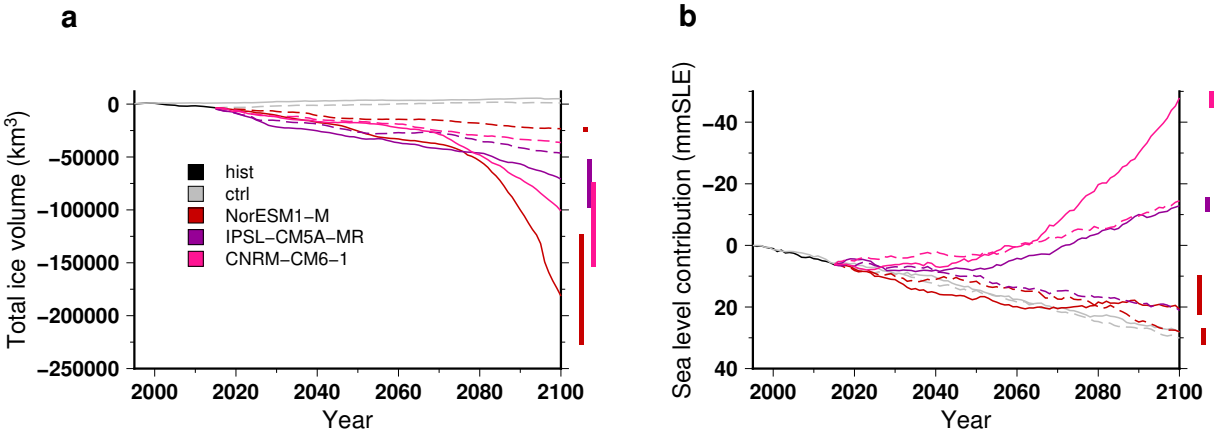

Figure 7. Simulated ice volume change for the historical experiment *hist* (1995-2015), the control experiments *ctrl* (solid grey lines) and *ctrl_proj* (dashed grey lines) and for the projections using climate models run under a pessimistic greenhouse scenario (solid lines, RCP8.5 for NorESM1-M and IPSL-CM5A-MR, and SSP585 for CNRM-CM6-1) and an optimistic greenhouse scenario (dashed lines, RCP2.6 for NorESM1-M and IPSL-CM5A-MR, and SSP126 for CNRM-CM6-1) with a medium oceanic sensitivity, expressed as: **(a)** total ice volume change and **(b)** ice volume contributing to sea level rise. For each projection experiment, the right-hand side vertical bar shows the minimal and maximal volume change associated with the oceanic forcing sensitivity to temperature change (*low* and *high*)

https://doi.org/10.5194/tc-2020-140
Preprint. Discussion started: 2 June 2020

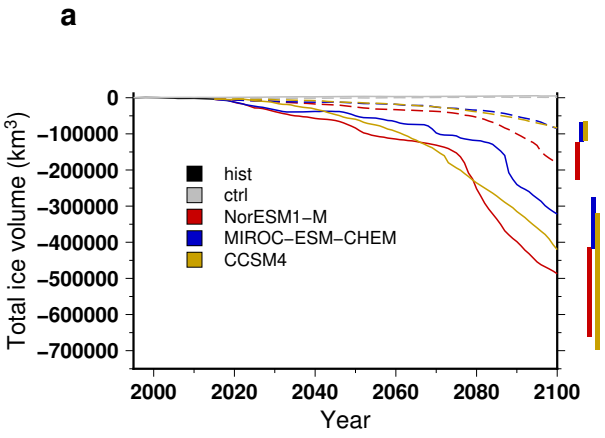

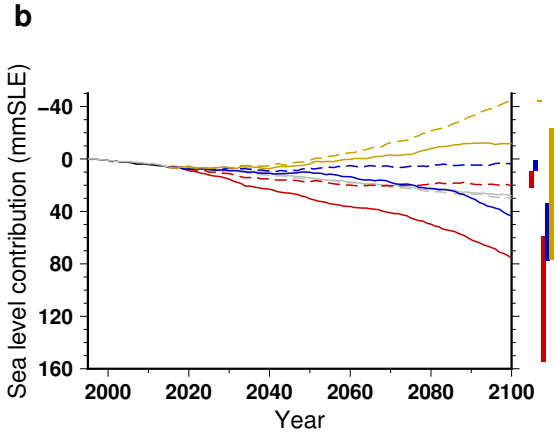

Figure 8. Simulated ice volume change for the historical experiment *hist* (1995-2015), the control experiment *ctrl_proj* (solid grey line) and the projections under different CMIP5 forcings using the RCP8.5 scenario and the medium oceanic sensitivity. For the projections, the solid lines stand for experiments that use a sub-shelf melting rate parametrisation calibrated against the Pine-Island glacier area only while the dashed lines stand for experiments that use the sub-shelf melting rate parametrisation calibrated against the Antarctic-wide dataset. The volume change is expressed as: **(a)** total ice volume change and **(b)** ice volume contributing to sea level rise. For each projection experiment the vertical bar shows the minimal and maximal volume change associated with the oceanic forcing sensitivity to temperature change (*low* and *high*).

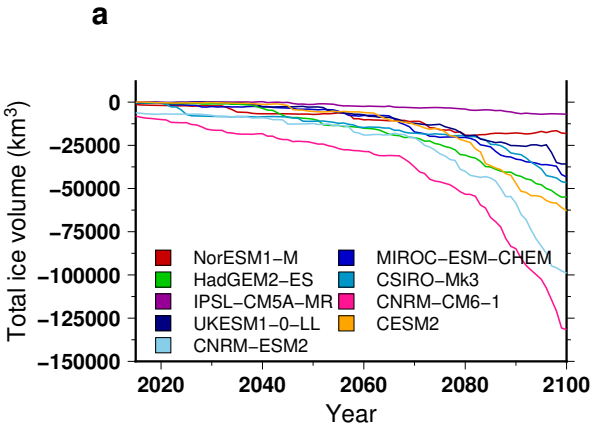

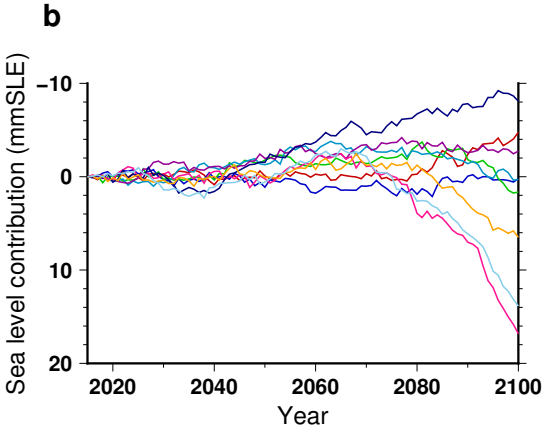

Figure 9. Simulated ice volume difference between the shelf collapse scenario (*SC*) and the standard approach for the projections under different CMIP5 and CMIP6 forcings using the RCP8.5 scenario and SSP585 scenario, respectively. The volume change is expressed as: **(a)** total ice volume change and **(b)** ice volume contributing to sea level rise. The projection experiments shown in this figure use the medium oceanic sensitivity.

https://doi.org/10.5194/tc-2020-140
Preprint. Discussion started: 2 June 2020

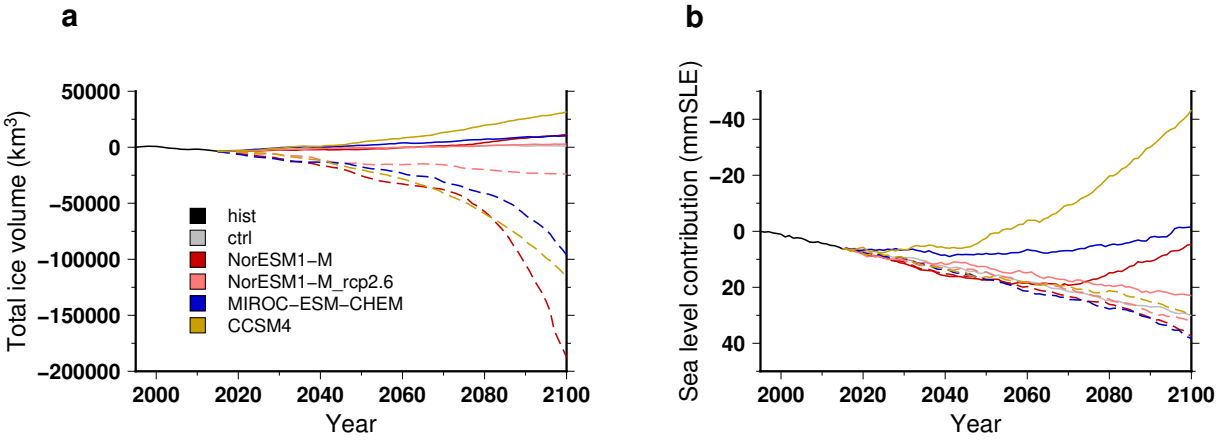

Figure 10. Simulated ice volume change for the historical experiment *hist* (1995-2015), the control experiment *ctrl_proj* (solid grey line) and the projections under different CMIP5 forcings using the RCP8.5 scenario. For the projections, the solid lines stand for experiments under atmospheric forcing change only (no change in sub-shelf melting rates) while the dashed lines stand for experiments under oceanic forcing change only (no change in surface mass balance nor surface temperature). The volume change is expressed as: **(a)** total ice volume change and **(b)** ice volume contributing to sea level rise. The projection experiments shown in this figure use the medium oceanic sensitivity.

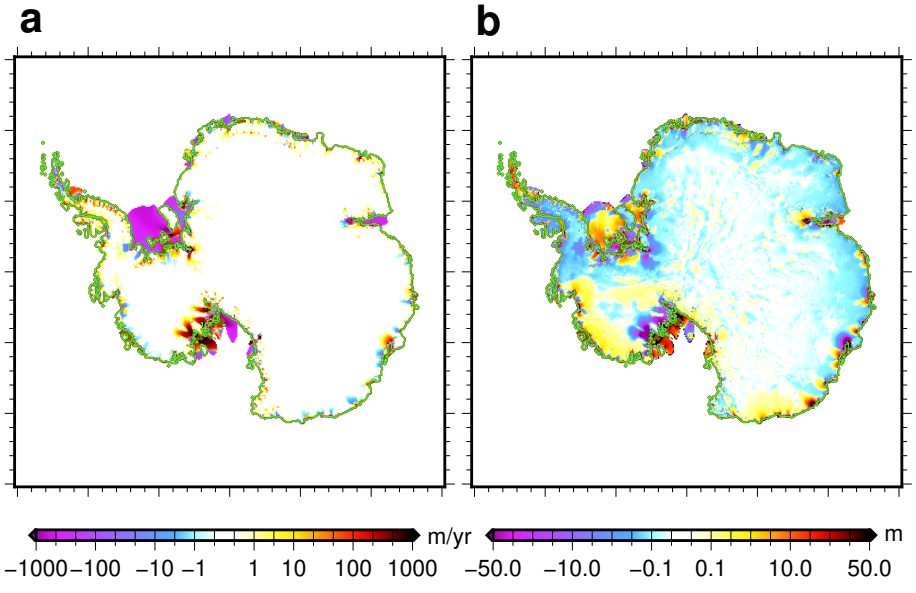

Figure 11. **(a)**: Simulated surface velocity change during the projection run (2096-2100 with respect to 2015-2019) using NorESM1-M forcing under RCP8.5 with a medium oceanic sensitivity. **(b)**: change in the dynamic contribution to ice thickness change in 2100 (see text for definition) for this same experiment. For both panel, we corrected the changes by the ones simulated in the control experiment *ctrl_proj* over the same period.

https://doi.org/10.5194/tc-2020-140
Preprint. Discussion started: 2 June 2020

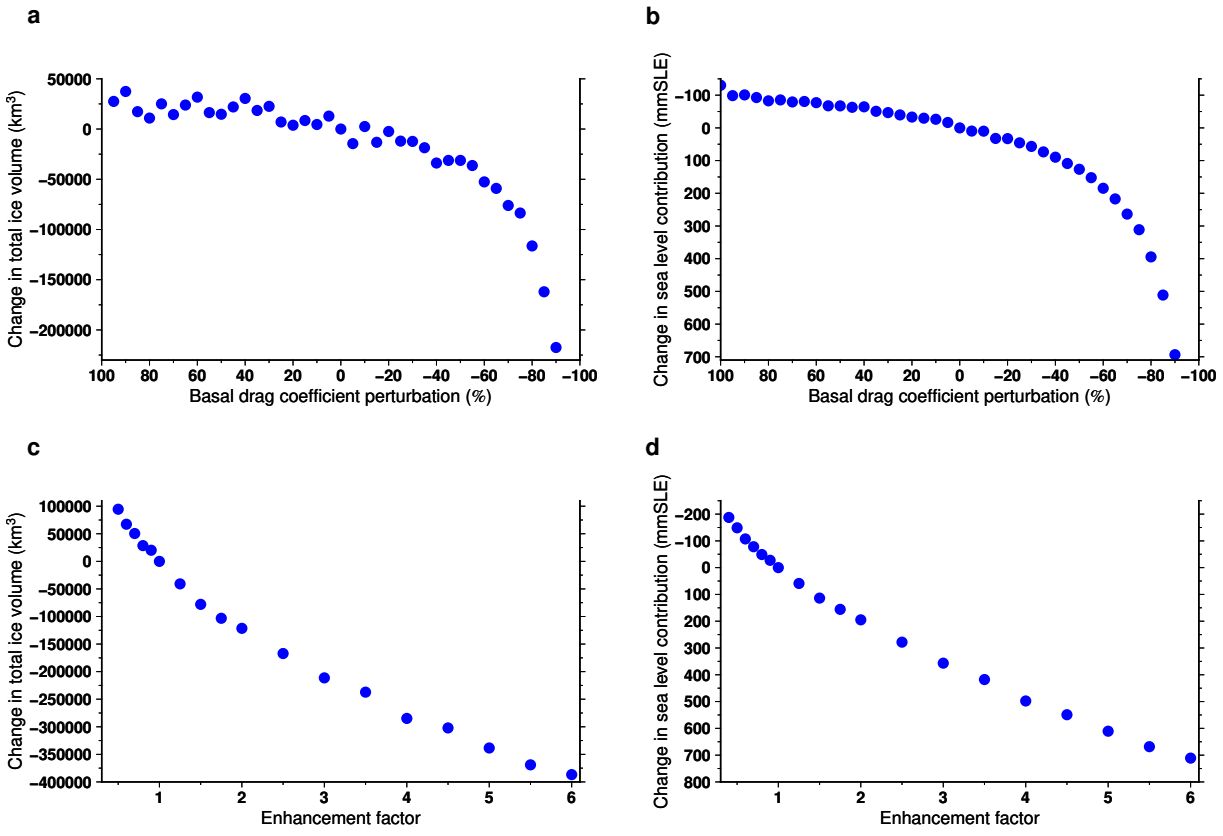

Figure 12. Change in ice volume for a modification of the basal drag coefficient ((**a**) and (**b**)) and different values of the enhancement factor ((**c**) and (**d**)). In this figure, each dot represents the ice volume difference in 2100 with respect to the standard projection experiment (zero basal drag coefficient perturbation and enhancement factor at 1). The climate forcing used for this figure is NorESM1-M under RCP8.5 with a medium oceanic sensitivity. The perturbation is applied starting at year 2045. The difference is expressed in total ice volume ((**a**) and (**c**)) and ice volume contributing to sea level rise ((**b**) and (**d**)).